Geometric Parameters in Nucleic Acids: Sugar and Phosphate Constituents

Anke Gelbin,[†] Bohdan Schneider,[†,‡] Lester Clowney,[†] Shu-Hsin Hsieh,[†] Wilma K. Olson,[†] and Helen M. Berman*,[†]

Contribution from the Department of Chemistry, Rutgers University, Piscataway, New Jersey 08855-0939, and J. Heyrovsky Institute of Physical Chemistry, The Academy of Sciences of the Czech Republic, 18223 Prague, Czech Republic

Received August 21, 1995[⊗]

Abstract: A statistical survey of the torsion angles, bond angles, and bond lengths in the sugar and phosphate groups of well-refined mononucleoside, mononucleotide, dinucleoside monophosphate, and trinucleoside diphosphate crystal structures contained in the Cambridge Structural Database and the Nucleic Acid Database is reported. The mean values of the geometrical parameters in these structures and their estimated standard deviations are separated according to their chemistry and conformation. These new parameters serve as a basis for a dictionary of standard nucleic acid geometry.

Introduction

A reliable set of standard nucleic acid geometries is critical both in molecular modeling and in the refinement and interpretation of structure in crystals containing nucleic acids. Since the resolution of these crystal structures is usually not atomic, refinement procedures require restraints on the covalent geometry and, on occasion, the torsion angles. Thus, it is important to define standardized geometric parameters for nucleic acids that can be introduced into the dictionaries used in various programs for crystallographic refinement as well as for empirical energy calculations.

The best source for defining the nucleic acid standards are the high-resolution small-molecule crystal structures contained in the Cambridge Structure Database (CSD)[1] and atomic resolution oligonucleotides in the Nucleic Acid Database (NDB).[2] A survey of bases reported in the accompanying article by Clowney *et al.*[3] reveals the significantly larger sample of nucleoside and nucleotide structures now at hand compared to those that were available when the existing set of base parameters was determined.[4] The relative size of the current sample compared to that used in earlier surveys of the sugar geometry is even more pronounced. Earlier studies were forced, from necessity, to include furanose rings other than ribose and 2′-deoxyribose in the determination of parameters. Even then, there were not sufficient data to describe the continuum of states associated with the interconversion, or pseudorotation, of the commonly puckered ring conformations.[5]

Unlike the base geometries, which do not have conformational dependence, the interrelationships between conformation and valence geometry in furanose rings are quite complex. The earliest crystallographic analyses of nucleoside and nucleotide structures revealed the consequences of sugar puckering on the bond lengths and angles of the furanose ring, most notably the decreased internal valence angle centered at the atom displaced from the main ring plane.[6,7] Further accumulation of structural examples identified the preferred conformations of the nucleic acid chain and led to various quantitative descriptions of the geometry of the furanose ring.[5,8−10] An early survey of 42 three-dimensional β-nucleoside and β-nucleotide sugars[11] yielded two sets of standard bond lengths and valence angles corresponding to the mean values in the two major conformations (C2′-*endo* or C3′-*endo*) where the ring is puckered at the C2′ or C3′ atom or both. These values were subsequently incorporated in many crystallographic refinement and modeling programs and have been widely used in the nucleic acid structures determined to date.

Later analysis of 60 β-nucleoside crystal structures led to the development of a function that related the valence angles of the sugars to their conformation.[12] The limited data sets were suggestive of the large flexibility of bond angles that, as shown here, is now completely revealed during the course of pseudorotation. Earlier theoretical estimations of the variation of bond lengths with ring puckering[13] are also now substantiated. In view of the increasing number of structure determinations of crystals containing nucleic acids, including protein−nucleic acid complexes, it is particularly appropriate to update the standard values for the geometry of both ribose and deoxyribose rings as a function of their conformation.

By contrast to the sugars, the data needed to determine accurate values for the geometry of the phosphodiester linkage are still rather sparse. A recent survey of the CSD has identified eight non-nucleotide compounds that contain this linkage.[14]

[†] Rutgers University.
[‡] The Academy of Sciences of the Czech Republic.
* To whom correspondence should be addressed.
[⊗] Abstract published in *Advance ACS Abstracts,* January 1, 1996.

(1) Allen, F. H.; Bellard, S.; Brice, M. D.; Cartright, B. A.; Doubleday, A.; Higgs, H.; Hummelink, T.; Hummelink-Peters, B. G.; Kennard, O.; Motherwell, W. D. S.; Rodgers, J. R.; Watson, D. G. *Acta Crystallogr.* **1979**, *B35*, 2331−2339.
(2) Berman, H. M.; Olson, W. K.; Beveridge, D. L.; Westbrook, J.; Gelbin, A.; Demeny, T.; Hsieh, S.-H.; Srinivasan, A. R.; Schneider, B. *Biophys. J.* **1992**, *63*, 751−759.
(3) Clowney, L.; Jain, S. C.; Srinivasan, A. R.; Westbrook, J.; Olson, W. K.; Berman, H. M. *J. Am. Chem. Soc.* **1996**, *118*, 509−518.
(4) Taylor, R.; Kennard, O. *J. Mol. Struct.* **1982**, *78*, 1−28.
(5) Altona, C.; Sundaralingam, M. *J. Am. Chem. Soc.* **1972**, *94*, 8205−8212.
(6) Sundaralingam, M. *J. Am. Chem. Soc.* **1965**, *87*, 599−606.
(7) Sundaralingam, M.; Jensen, L. H. *J. Mol. Biol.* **1965**, *13*, 914.
(8) Sundaralingam, M. *Biopolymers* **1969**, *7*, 821−860.
(9) Cremer, D.; Pople, J. A. *J. Am. Chem. Soc.* **1975**, *97*, 1354−1358.
(10) Marzec, C. J.; Day, L. A. *Biomol. Struct. Dyn.* **1993**, *10*, 1091−1123.
(11) Arnott, S.; Hukins, D. W. L. *Biochem. J.* **1972**, *130*, 453−465.
(12) Murray-Rust, P.; Motherwell, S. *Acta Crystallogr.* **1978**, *B34*, 2534−2546.
(13) Pearlman, D. A.; Kim, S.-H. *J. Biomol. Struct. Dyn.* **1985**, *3*, 85−98.
(14) Kabelac, M.; Hobza, P.; Schneider, B. Manuscript in preparation.

0002-7863/96/1518-0519$12.00/0

Table 1. CSD Codes of Mononucleoside and Mononucleotide Structures[a]

fikhai	docytc	keclot	admpot10	cytidn	kurdpi
fikhai01	doxadm	medour	adoshc	demxey	leuaur10
foylua	duhhuj	pryurd10	adposm	dmguan10	meurid
fuxbij	dumtou	sdgunp	adposm01	dmurid	meyrid
gexxiq	dxcytd	sifgap	berhah	erfimp	mguosm
gexxiq01	etyxur	thydin	beurid10	fucwij	mguosm01
gidtes	gebtem	vdurid	bguaos10	gicmou	mxurid01
jafhih	gergal	vexdor	bimfim10	guanph01	palaur10
acurid	geycao	acados	caxwih	guansh10	pctrib10
boxgie	geyces	adposd	cbmurd	guopna10	pucglr10
cezbis	gidtiw	cytiac	cekluz	guopna11	sekxip10
cezfoc	gojwor	cytiac01	citxos10	guosbh	selzis
cezmez	hmdour	daurid01	coczid	hxurid	suromm
dadpnh10	ipdxur	suridp	cupyuh	jawjia	taljar
defpot	jappev	uridmp10	cxmurd	jigcux	toaden
docypo	jibdih	adenos01	cyticl	kadphd02	uroame
docypo02	jubvil	adenos10	cytidi01	kehzay	vuymad
docypo03	jubvor	admopm	cytidi10	kivhom	xantos

[a] The references for these structures are available on the WWW (http://ndbserver.rutgers.edu) in the Archives Section.

However, the most appropriate models for the identification of nucleic acid standards are the very high-resolution structures of small fragments of nucleic acids. Although the number of these high resolution oligomers is small, it may be sufficient to obtain meaningful standard numbers.

Here we present an analysis of ribose and deoxyribose sugars from over 100 well-determined crystal structures. Because the number of examples is now large enough, it is possible to use fragments that are more representative of nucleic acids. Hence, only deoxyribose and ribose sugars have been included. We also present a survey of the phosphodiester linkages in well-determined short oligonucleotides and report the resultant valence geometries and ranges of torsion angles in the sugar−phosphate backbones.

Methods

Selection Criteria. The CSD[1] was searched for mononucleoside and mononucleotide crystal structures suitable for an investigation of the geometry of the nucleic acid sugar ring. A total of 64 ribose and 44 deoxyribose high-resolution mononucleotide and mononucleoside crystal structures were selected (Table 1). Because many of the crystals contain more than one molecule in the asymmetric unit, the search yielded 80 ribose sugars and 47 deoxyribose sugars. Only structures with R values below 0.08 and average estimated standard deviations (esd) of the C−C bond lengths no greater than 0.02 Å were included. The majority of structures had esd's closer to 0.01 Å.

The structures in the survey contain the common bases—guanine, adenine, cytosine, thymine, or uracil—with standard β-glycosyl linkages (C1′−N9 for purines and C1′−N1 for pyrimidines) to the attached sugars. Acetic acid modifications of the 3′ or 5′ oxygens and diphosphate sugars are accepted. All structures with halogen modified bases and with atoms of atomic number greater than 20 are excluded. For the purpose of this analysis only, the selected structures have been placed in a relational database similar to the NDB.[15]

Well-refined dinucleoside phosphates from the NDB were used to investigate the behavior of the acyclic backbone torsion angles and the bond lengths and valence angles of the phosphodiester linkage. The structures of nine dinucleoside phosphate structures and one trinucleoside diphosphate structure, all of which were refined by full matrix least squares to a crystallographic R factor below 0.08 (Table 2), were selected.

Analyses. Graphical representations and tables of the derived structural information, including bond lengths, valence bond angles, and torsion angles, were created and analyzed using the NDB software.[2]

(15) Berman, H. M., Westbrook, J., Clowney, L., Gelbin, A., Hsieh, S.-H. Manuscript in preparation.

Table 2. NDB Codes of Dinucleoside Monophosphate and Trinucleoside Diphosphate Structures[a]

arb002	udb004	urb001	urb008	urb020
drb003	udb005	urb003	urb016	urc002

[a] The references for these structures are available on the WWW (http://ndbserver.rutgers.edu) in the Archives Section.

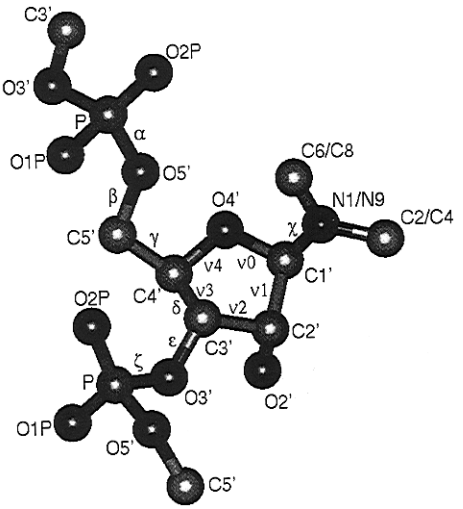

Figure 1. Atomic labeling and definitions of torsion angles for nucleotides. The torsion angles are defined as follows: ν_0, C4′−O4′−C1′−C2′; ν_1, O4′−C1′−C2′−C3′; ν_2, C1′−C2′−C3′−C4′; ν_3, C2′−C3′−C4′−O4′; ν_4, C3′−C4′−O4′−C1′; α, O3′−P−O5′−C5′; β, P−O5′−C5′−C4′, γ: O5′−C5′−C4′−C3′, δ: C5′−C4′−C3′−O3′, ϵ: C4′−C3′−O3′−P, ζ: C3′−O3′−P−O5′; χ, O4′−C1′−N1−C2 (pyrimidines) and O4′−C1′−N9−C4 (purines).

The geometric parameters were compared against previously determined standard values. The mean values of sugar parameters were compared with earlier surveys of furanose rings in mononucleosides, mononucleotides, and dinucleoside phosphates[11] and of β-1′-amino-furanosides.[12] The mean values of the phosphate bond lengths and angles were compared against those determined previously for all organic molecules[16] and those recently found for non-nucleotide compounds containing phosphodiester linkages.[14]

A series of statistical tests was used to compare various parameters in pairings of ring conformation and sugar chemistry. Because distributions with significantly different esd's cannot be compared by Student's t test, the F test was used to compare the equality of variances. In cases where the esd's of the distributions were significantly different, the Fisher−Behrens t test, a modification of Student's t test,[17] was employed to compare the means of sample sets and also to determine whether two subgroups of structures form separate classes. The probability, P_t, that a common mean is shared by two samples is the significance level for this test. Two means were called significantly different when the probability was below 5%.

Results

The results of these analyses are reported separately for the sugar and phosphodiester backbone groups. The atomic labeling and definitions of torsion angles are given in Figure 1. Figure 2 illustrates the commonly preferred C3′-*endo* and C2′-*endo* sugar puckering modes of the furanose ring found in nucleosides and nucleotides. In these two examples, the designated atom is displaced out of the mean four-atom plane of the furanose ring and is located on the same side as the C5′ atom. This figure also contains the definitions of the pseudorotational parameters, P and ν_{max}, that are commonly used to describe

(16) Allen, F. H.; Kennard, O.; Watson, D. G.; Brammer, L.; Orpen, A. G.; Taylor, R. *J. Chem. Soc., Perkin Trans. 2* **1987**, S1−S19.

(17) Hamilton, W. *Statistics in Physical Science*; Ronald Press: New York, 1964; pp 92−94.

Table 3. Comparison of Bond Lengths in Furanose Rings

	ribose and deoxyribose						
bond	$\bar{x}_R$[a]	$\bar{x}_D$[b]	$P_{t\,S}$[c]	σ_R,[a] N[d]	σ_D,[b] N	$\bar{x}_{AH}$[e]	σ_{AH},[e] N
C1′−C2′	1.528	1.521	0.004	0.010, 80	0.014, 47	1.525	0.017, 39
C2′−C3′	1.525	1.518	0.000	0.011, 80	0.010, 47	1.528	0.019, 38
C3′−C4′	1.524	1.528	0.038	0.011, 80	0.010, 47	1.529	0.021, 41
C4′−O4′	1.453	1.446	0.001	0.012, 80	0.011, 47	1.457	0.020, 41
O4′−C1′	1.414	1.420	0.011	0.012, 80	0.013, 47	1.419	0.023, 40
C3′−O3′	1.423	1.431	0.002	0.014, 80	0.013, 47	1.422	0.021, 41
C5′−C4′	1.510	1.511	0.593	0.013, 80	0.008, 47	1.516	0.022, 40
C2′−O2′	1.413	na	na	0.013, 80	na	1.417	0.019, 42
C1′−N1/N9	1.471	1.474	0.391	0.017, 80	0.020, 47	1.465[f]	0.019, 21
C1′−N1/N9						1.490[g]	0.018, 21
(H)O5′−C5′	1.423	1.420	0.444	0.014, 61	0.021, 37	na	na

	C2′-*endo*					C3′-*endo*					C2′- vs C3′-*endo*	
bond	$\bar{x}_R$	$\bar{x}_D$	$P_{t\,C2}$[h]	σ_R, N	σ_D, N	$\bar{x}_R$	$\bar{x}_D$	$P_{t\,C3}$[i]	σ_R, N	σ_D, N	$P_{t\,R}$[j]	$P_{t\,D}$[k]
C1′−C2′	1.526	1.518	0.001	0.008, 49	0.010, 29	1.529	1.519	0.042	0.011, 24	0.010, 7	0.241	0.817
C2′−C3′	1.525	1.516	0.000	0.011, 49	0.008, 29	1.523	1.518	0.346	0.011, 24	0.012, 7	0.469	0.686
C3′−C4′	1.527	1.529	0.414	0.011, 49	0.010, 29	1.521	1.521	1.000	0.010, 24	0.010, 7	0.024	0.063
C4′−O4′	1.454	1.446	0.001	0.010, 49	0.010, 29	1.451	1.449	0.649	0.013, 24	0.009, 7	0.326	0.455
O4′−C1′	1.415	1.420	0.065	0.012, 49	0.011, 29	1.412	1.418	0.276	0.013, 24	0.012, 7	0.347	0.696
C3′−O3′	1.427	1.435	0.009	0.012, 49	0.013, 29	1.417	1.419	0.588	0.014, 24	0.006, 7	0.005	0.000
C5′−C4′	1.509	1.512	0.167	0.012, 49	0.007, 29	1.508	1.509	0.826	0.007, 24	0.011, 7	0.655	0.627
C2′−O2′	1.412	na	na	0.013, 49	na	1.420	na	na	0.010, 24	na	0.005	na
C1′−N1/N9	1.464	1.468	0.227	0.014, 49	0.014, 29	1.483	1.488	0.404	0.015, 24	0.013, 7	0.000	0.004
(H)O5′−C5′	1.424	1.418	0.296	0.016, 36	0.025, 25	1.420	1.423	0.531	0.009, 20	0.011, 7	0.449	0.236

[a] $\bar{x}_R$, mean value (Å) of ribose bond distance; σ_R, esd of ribose bond distance. [b] $\bar{x}_D$, mean value (Å) of deoxyribose bond distance; σ_D, esd of deoxyribose bond distance. [c] $P_{t\,S}$, significance level of *t* test for comparison of ribose and deoxyribose sugars. [d] N, sample size. [e] $\bar{x}_{AH}$, mean value (Å) given by Arnott and Hukins;[11] σ_{AH}, esd of Arnott and Hukins parameter. [f] C2′-*endo* conformers. [g] C3′-*endo* and C3′-*exo* conformers. [h] $P_{t\,C2'}$, significance level of *t* test for comparison of C2′-*endo* ribose and deoxyribose sugars. [i] $P_{t\,C3'}$, significance level of *t* test for comparison of C3′-*endo* ribose and deoxyribose sugars. [j] $P_{t\,R}$, significance level of *t* test for comparison of C2′-*endo* and C3′-*endo* ribose sugars. [k] $P_{t\,D}$, significance level of *t* test for comparison of C2′-*endo* and C3′-*endo* deoxyribose sugars.

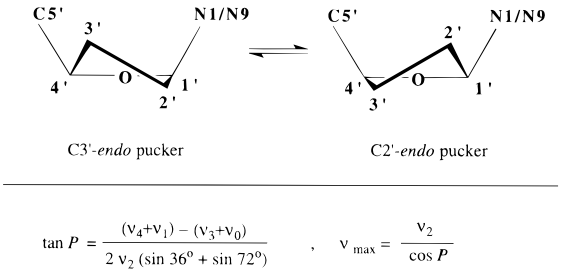

Figure 2. Schematic drawing of the preferred sugar puckering modes of the furanose ring found in nucleotides and nucleosides and definition of pseudorotation phase angle P and puckering amplitude ν_{max}.[5]

the conformational state of the sugar within the continuum of puckered states.[5,18,19] The C3′-*endo* state lies in the so-called N range of pseudorotational values, $0° \le P \le 36°$, and the C2′-*endo* state is in the S range, $144° \le P \le 190°$.[5] Here we use the terms C3′-*endo* and C2′-*endo* to represent these ranges, rather than the narrower set of specifically puckered states.

Pseudorotational States. Because it has already been established that the valence geometry is dependent on sugar conformation,[11,12] it was necessary to establish how to best divide the current sample into appropriate conformational ranges. The distribution of P for the mononucleosides and mononucleotides in this survey is shown in Figure 3a. Out of the 127 structures in the sample, 78 structures are in the C2′-*endo* range, 31 lie in the C3′-*endo* range, and 18 do not belong to either conformational group. The pseudorotation amplitude ν_{max}[5,20−22] is reported as a function of P in Figure 3b. Its value is somewhat variable and lower on average than the mean value of 38.7° found in earlier studies of nucleotides and nucleosides.[5]

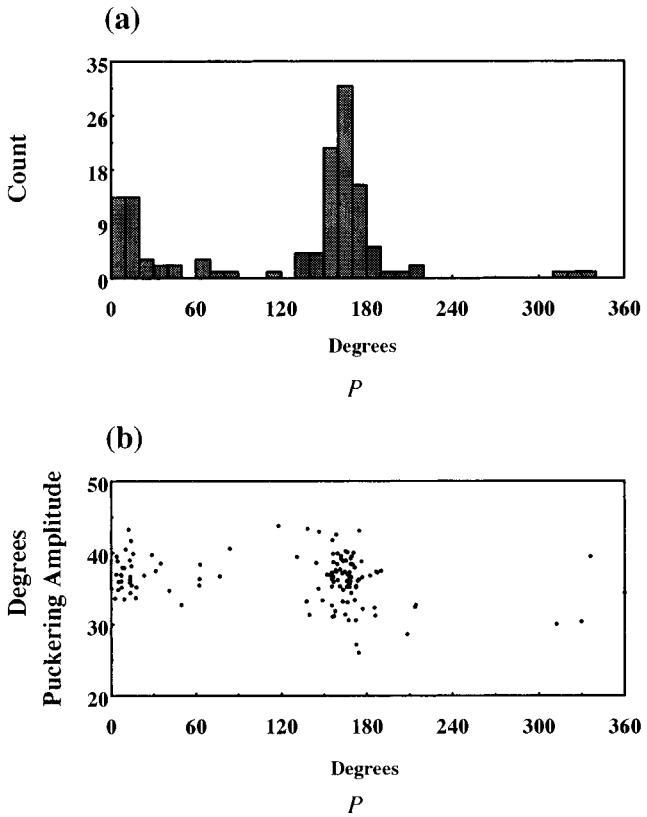

Figure 3. (a) Distribution histogram, in 10° intervals, of the pseudorotation phase angle P observed in mononucleosides and mononucleotides. (b) Scattergram displaying puckering amplitude ν_{max}, in degrees, versus P in degrees for all structures included in the search.

(18) Kilpatrick, J. E.; Pitzer, K. S.; Spitzer, R. *J. Am. Chem. Soc.* **1947**, *69*, 2483−2488.
(19) Hall, L. D.; Steiner, P. R.; Pedersen, C. *Can. J. Chem.* **1970**, *48*, 1155−1165.
(20) Westhof, E.; Sundaralingam, M. *J. Am. Chem. Soc.* **1980**, *102*, 1493−1500.

Table 4. Comparison of Bond Angles in Furanose Rings

	ribose and deoxyribose								
angle	$\bar{x}_R$[a]	$\bar{x}_D$[b]	$P_{t\,S}$[c]	σ_R,[a] N	σ_D,[b] N	$\bar{x}_{AH\text{-}C2'}$[d]	$\sigma_{AH\text{-}C2'}$,[d] N	$\bar{x}_{AH\text{-}C3'}$[e]	$\sigma_{AH\text{-}C3'}$,[e] N
C1′−C2′−C3′	101.5	102.7	0.000	0.9, 80	1.4, 47	101.4	2.4, 42	101.4	2.4, 42
C2′−C3′−C4′	102.7	103.2	0.008	1.0, 80	1.0, 47	102.5	1.9, 42	102.5	1.9, 42
C3′−C4′−O4′	105.5	105.6	0.641	1.4, 80	1.0, 47	105.5	1.7, 19	104.0	1.8, 16
C4′−O4′−C1′	109.6	109.7	0.662	0.9, 80	1.4, 47	109.7	1.0, 17	109.7	1.0, 17
O4′−C1′−C2′	106.4	106.1	0.183	1.4, 80	1.1, 47	105.6	1.3, 19	106.9	3.0, 14
C1′−C2′−O2′	110.6	na	na	3.0, 80	na	112.5	2.4, 20	na	na
C3′−C2′−O2′	113.3	na	na	2.9, 80	na	114.6	2.7, 19	110.8	1.9, 17
C2′−C3′−O3′	111.0	110.6	0.428	2.8, 80	2.7, 47	109.3[f]	2.3, 22	113.3	2.5, 17
C4′−C3′−O3′	110.6	110.3	0.490	2.6, 80	2.2, 47	108.9	2.7, 20	111.9[g]	2.4, 20
C5′−C4′−C3′	115.5	114.7	0.005	1.5, 80	1.5, 47	115.8	2.7, 42	115.8	2.7, 42
C5′−C4′−O4′	109.2	109.4	0.479	1.4, 80	1.6, 47	108.9	2.0, 42	108.9	2.0, 42
O4′−C1′−N1/N9	108.2	107.8	0.015	1.0, 80	0.8, 47	108.0	1.8, 42	108.0	1.8, 42
C2′−C1′−N1/N9	113.4	114.2	0.008	1.6, 80	1.6, 47	113.7	2.7, 42	113.7	2.7, 42
(H)O5′−C5′−C4′	111.6	110.9	0.080	1.7, 61	2.0, 37	na	na	na	na
C1′−N9−C4[h]	127.1	125.9	0.017	1.8, 46	1.4, 13	na	na	na	na
C1′−N1−C2[i]	117.9	117.8	0.761	1.3, 34	1.4, 34	na	na	na	na

	C2′-*endo*					C3′-*endo*					C2′ vs C3′-*endo*	
angle	$\bar{x}_R$	$\bar{x}_D$	$P_{t\,C2'}$[j]	σ_R, N	σ_D, N	$\bar{x}_R$	$\bar{x}_D$	$P_{t\,C3'}$[k]	σ_R, N	σ_D, N	$P_{t\,R}$[l]	$P_{t\,D}$[m]
C1′−C2′−C3′	101.5	102.5	0.000	0.8, 49	1.2, 29	101.3	102.4	0.008	0.7, 24	0.8, 7	0.279	0.794
C2′−C3′−C4′	102.6	103.1	0.026	1.0, 49	0.9, 29	102.6	102.2	0.248	1.0, 24	0.7, 7	1.000	0.013
C3′−C4′−O4′	106.1	106.0	0.533	0.8, 49	0.6, 29	104.0	104.5	0.059	1.0, 24	0.4, 7	0.000	0.000
C4′−O4′−C1′	109.7	110.1	0.064	0.7, 49	1.0, 29	109.9	110.3	0.221	0.8, 24	0.7, 7	0.302	0.546
O4′−C1′−C2′	105.8	105.9	0.629	1.0, 49	0.8, 29	107.6	106.8	0.006	0.9, 24	0.5, 7	0.000	0.002
C1′−C2′−O2′	111.8	na	na	2.6, 49	na	108.4	na	na	2.4, 24	na	0.000	na
C3′−C2′−O2′	114.6	na	na	2.2, 49	na	110.7	na	na	2.1, 24	na	0.000	na
C2′−C3′−O3′	109.5	109.4	0.859	2.2, 49	2.5, 29	113.7	112.6	0.421	1.6, 24	3.3, 7	0.000	0.042
C4′−C3′−O3′	109.4	109.7	0.590	2.1, 49	2.5, 29	113.0	112.3	0.432	2.0, 24	2.0, 7	0.000	0.012
C5′−C4′−C3′	115.2	114.1	0.007	1.4, 49	1.8, 29	116.0	115.7	0.599	1.6, 24	1.2, 7	0.043	0.012
C5′−C4′−O4′	109.1	109.3	0.314	1.2, 49	1.9, 29	109.8	109.8	1.000	0.9, 24	1.1, 7	0.007	0.589
O4′−C1′−N1/N9	108.2	108.0	0.252	0.8, 49	0.7, 29	108.5	108.3	0.282	0.7, 24	0.3, 7	0.107	0.093
C2′−C1′−N1/N9	114.0	114.3	0.352	1.3, 49	1.4, 29	112.0	112.6	0.449	1.1, 24	1.9, 7	0.000	0.056
(H)O5′−C5′−C4′	111.7	110.9	0.090	1.9, 36	1.7, 25	111.5	111.0	0.633	1.6, 20	2.5, 7	0.677	0.923
C1′−N9−C4[h]	127.4	126.3	0.055	1.2, 28	1.2, 7	126.3	123.9	0.051	2.8, 12	1.0, 2	0.213	0.052
C1′−N1−C2[i]	118.5	117.8	0.131	1.1, 21	1.8, 22	116.7	117.5	0.274	0.6, 12	1.4, 5	0.000	0.692

[a] $\bar{x}_R$, mean value (deg) of ribose bond angle; σ_R, esd of ribose bond angle. [b] $\bar{x}_D$, mean value (deg) of deoxyribose bond angle; σ_D, esd of deoxyribose bond angle. [c] $P_{t\,S}$, significance level of *t* test for comparison of ribose and deoxyribose sugars. [d] $\bar{x}_{AH\text{-}C2'}$, mean value (deg) of C2′-*endo* conformers given by Arnott and Hukins;[11] $\sigma_{AH\text{-}C2'}$, esd of Arnott and Hukins parameter of C2′-*endo* conformers. [e] $\bar{x}_{AH\text{-}C3'}$, mean value (deg) of C3′-*endo* conformers given by Arnott and Hukins;[11] $\sigma_{AH\text{-}C3'}$, esd of Arnott and Hukins parameter of C3′-*endo* conformers. [f] C2′-*endo* and C3′-*exo*. [g] C3′-*endo* and C3′-*exo*. [h] Purine. [i] Pyrimidine. [j] $P_{t\,C2'}$, significance level of *t* test for comparison of C2′-*endo* ribose and deoxyribose sugars. [k] $P_{t\,C3'}$, significance level of *t* test for comparison of C3′-*endo* ribose and deoxyribose sugars. [l] $P_{t\,R}$, significance level of *t* test for comparison of C2′-*endo* and C3′-*endo* ribose sugars. [m] $P_{t\,D}$, significance level of *t* test for comparison of C2′-*endo* and C3′-*endo* deoxyribose sugars.

The mean value of ν_{max} is 36.2° (3.3°) for the C2′-*endo*-like structures and 37.3° (2.4°) for the C3′-*endo*-like structures, where the numbers in parentheses are the standard deviations. The puckering amplitude is more variable in the C2′-*endo* family of structures with ring flattening observed for a few cases. In general, the deoxyribose sugars are slightly flatter than the ribose sugars, with $\nu_{max} = 35.2°$ for deoxyribose and 37.1° for ribose. The structures in this analysis were not categorized on the basis of puckering amplitude, and no structure was excluded because of an unusual value of ν_{max}.

Valence Geometry of the Deoxyribose/Ribose Groups. The sugar valence geometries were analyzed and compared for four groups of structures: ribose/C2′-*endo*, ribose/C3′-*endo*, deoxyribose/C2′-*endo*, and deoxyribose/C3′-*endo*. The bond lengths are tabulated in Table 3 and the valence angles in Table 4.

Bond Lengths. Although the histograms of the observed bond distances in all mononucleotides and mononucleosides appear unimodal (Figure 4), statistical analyses demonstrate that there are significant differences between the mean values of corresponding bond lengths in deoxyribose and ribose sugars. Only the C5′−C4′, C1′−N1/N9, and O5′−C5′ bond lengths do not depend on sugar chemistry. The 2′-deoxyribose and ribose parameters were further subdivided according to sugar conformation (Table 3) (bottom). Within the C2′-*endo* group of sugars, the C1′−C2′, C2′−C3′, C4′−O4′, and C3′−O3′ bond lengths differ significantly for deoxyribose or ribose sugars. In sugars with C3′-*endo* conformations, only the C1′−C2′ bond is different for ribose and deoxyribose.

Scattergrams, in which the covalent distances in the sugar ring are plotted as a function of the pseudorotation angle *P* (Figure 5), corroborate earlier predictions of the limited but slightly sinusoidal conformational dependence of the bond distances.[6,13] These scattergrams and a set of statistical tests, which compare all deoxyribose and ribose sugars as a function of their sugar pucker (Table 3 (bottom)), show that there is a pronounced conformational effect on the C3′−C4′, C3′−O3′, C2′−O2′, and C1′−N1/N9 bond lengths. The C3′−O3′ bond of the deoxyribose sugars is longer by 0.016 Å in the C2′-*endo* range, where the O3′ atom is in a pseudoequatorial position relative to the ribose ring. The observed conformational

(21) Sundaralingam, M.; Westhof, E. In *Proceedings of the Second SUNYA Conversation in the Discipline Biomolecular Stereodynamics*; Sarma, R. H., Ed.; Adenine Press: New York, 1981; Vol. 1, pp 301−325.

(22) De Leeuw, H. P. M.; Haasnoot, A. G.; Altona, C. *Isr. J. Chem.* **1980**, *20*, 108−126.

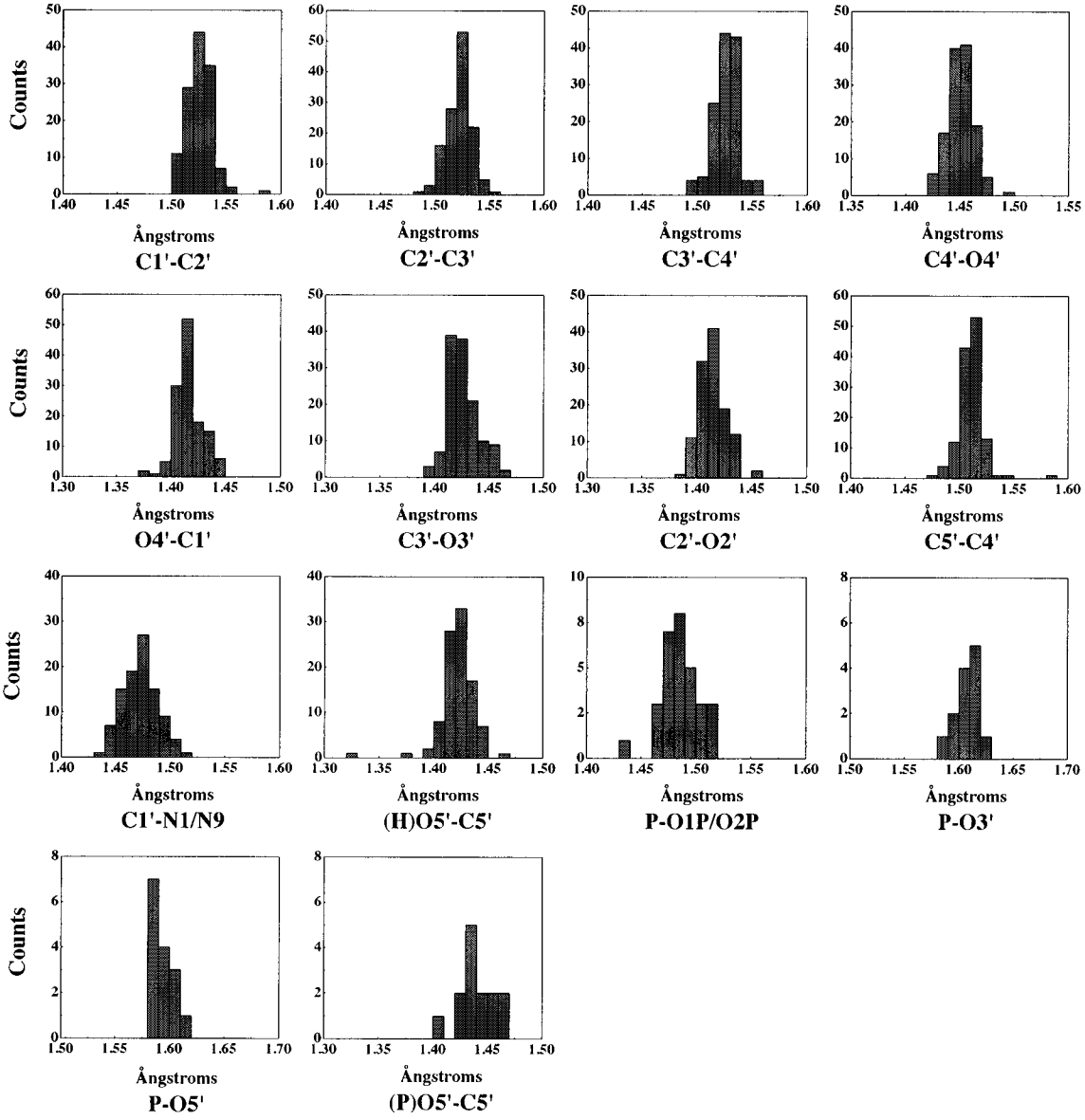

Figure 4. Histograms, in 0.01 Å intervals, of bond distances in the sugar ring and phosphodiester linkage. The distributions of bond lengths in the sugar ring are based on 127 mononucleotide and mononucleoside structures. The (H)O5′−C5′ bond length is calculated, using 99 mononucleosides. The bond lengths involving phosphorus are based on 10 di- and trinucleotides.

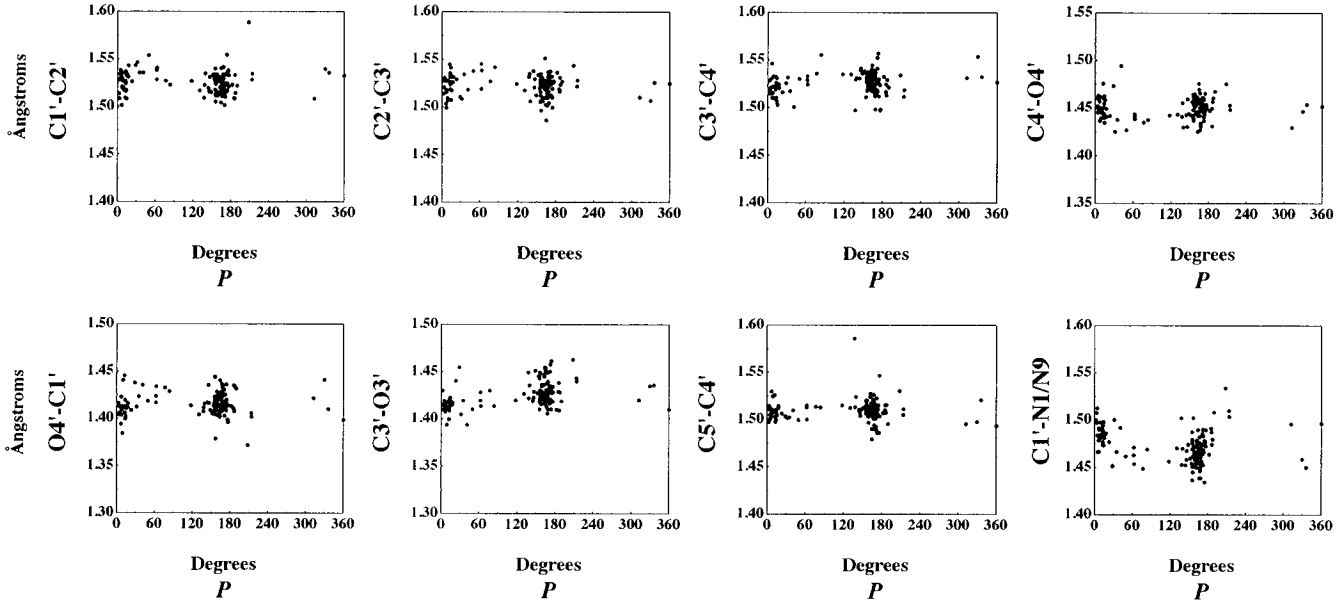

Figure 5. Scattergrams of bond distances, in angstroms, in the sugar ring versus pseudorotation phase angle *P* in degrees (for 127 mononucleotides and mononucleosides).

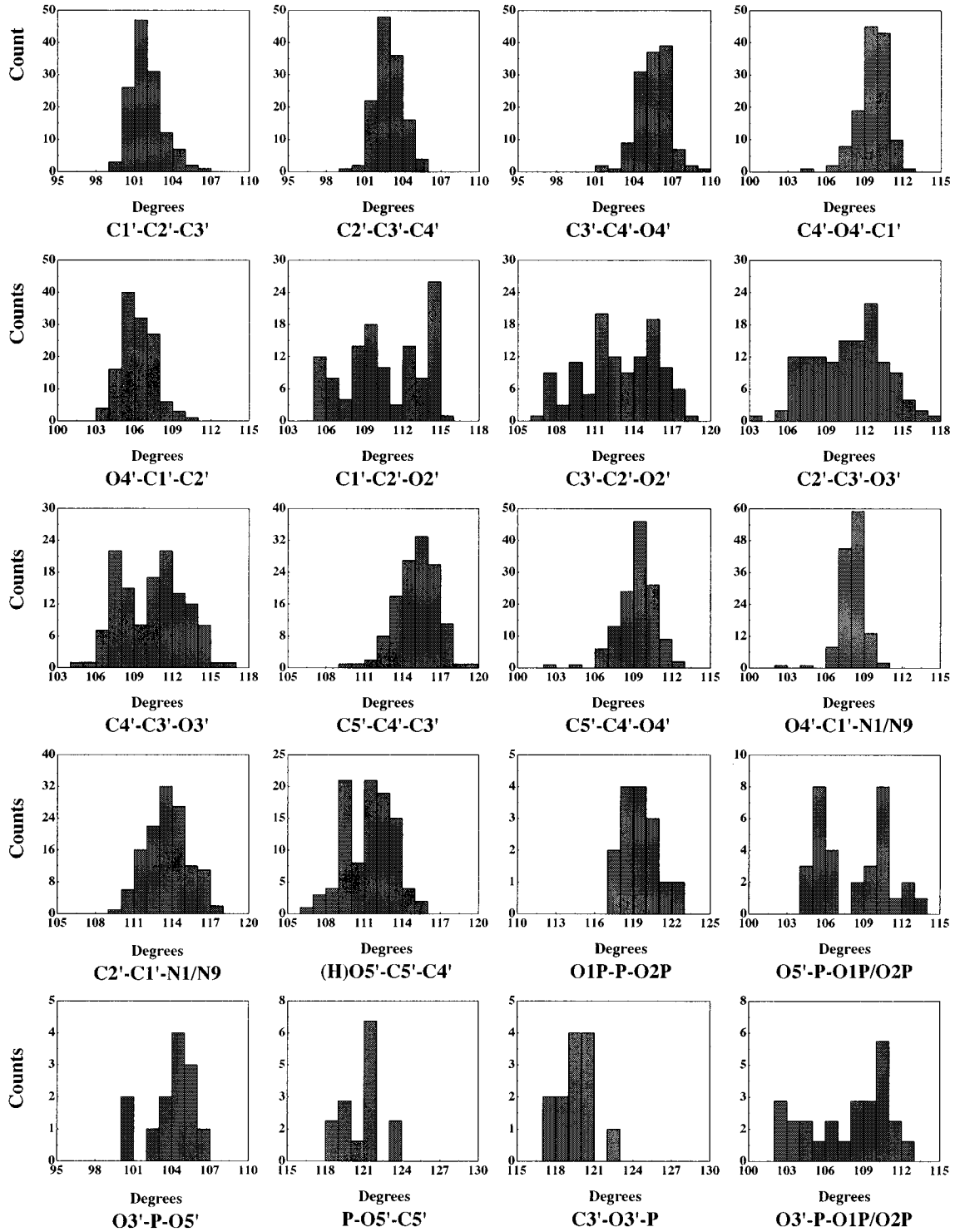

Figure 6. Histograms, in 1° intervals, of valence angles in the sugar ring and the phosphodiester linkage. The distributions of bond angles in the sugar ring are based on 127 mononucleotide and mononucleoside structures. The (H)O5′−C5′−C4′ bond angle was calculated using 99 mononucleosides. The bond angles involving phosphorus are based on 10 di- and trinucleotides.

dependence of the exocyclic C−O bonds confirms the earliest known predictions.[6]

The mean distances derived for the sample containing all furanose sugars show no significant differences from those derived in 1978 by Arnott and Hukins[11] with a much smaller sample set (≤42) and larger esd's (Table 3 (top)). In that study, a distinct dependency on sugar conformation was seen only for the glycosyl bond distance.

Valence Angles. Statistical results of the survey of the exo- and endocyclic sugar valence angles are summarized in Table 4. The broad distributions of valence angles in all structures are shown in Figure 6 and the scattergrams of the angles as a function of pseudorotation phase angle in Figure 7.

Statistical analyses demonstrate that the C1′−C2′−C3′, C2′−C3′−C4′, C5′−C4′−C3′, O4′−C1′−N1/N9, C2′−C1′−N1/N9, and C1′−N9−C4 angles are different in ribose and deoxyribose sugars regardless of sugar conformation (Table 4). If the sugars are further subdivided according to sugar conformation only three angles—C1′−C2′−C3′, C2′−C3′−C4′, and C5′−C4′−C3′—within the C2′-*endo* group depend on whether the sugar is ribose or deoxyribose. For C3′-*endo*-like sugars, only the

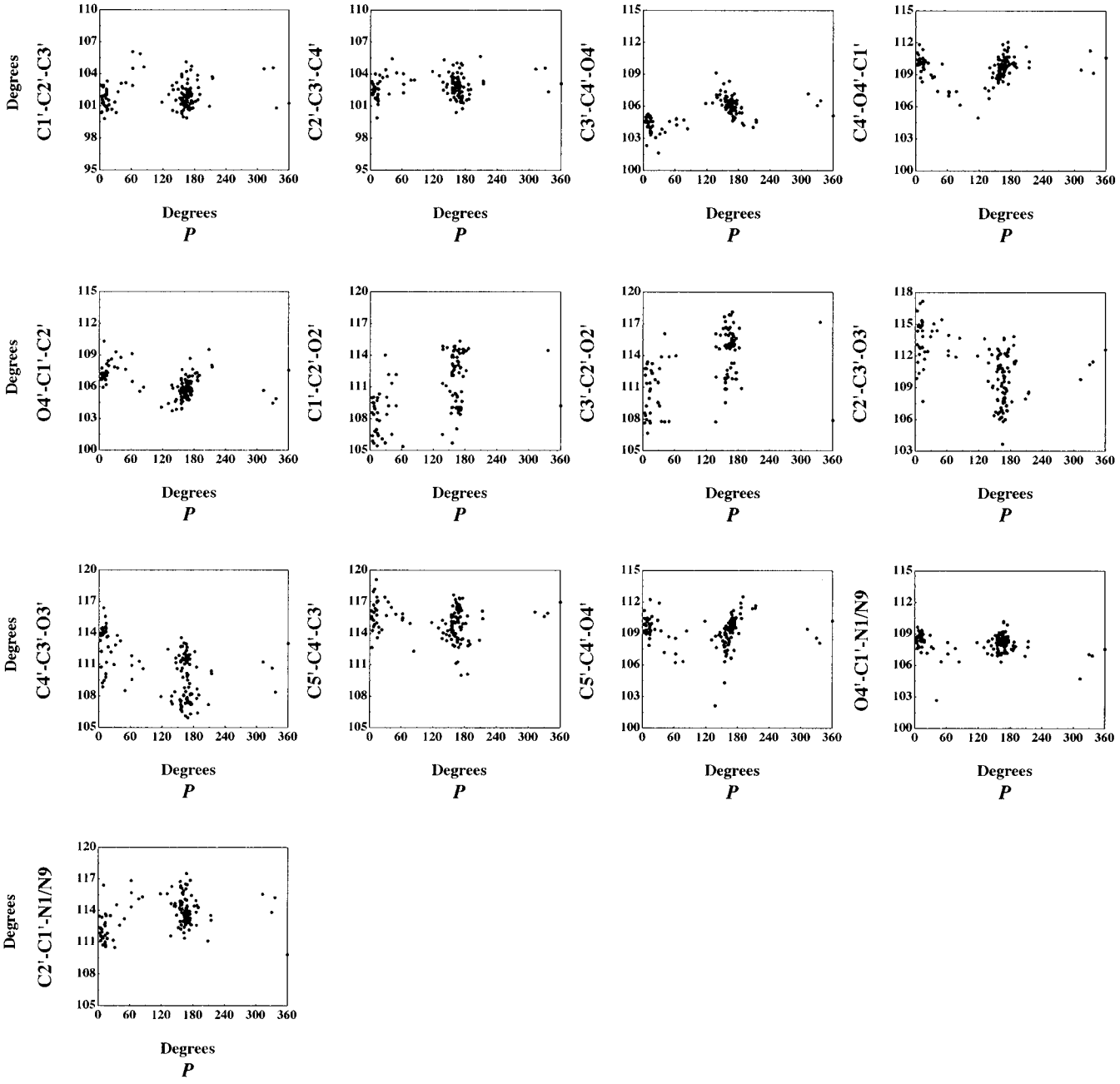

Figure 7. Scattergrams of sugar valence angles, in degrees, versus pseudorotation phase angle *P*, in degrees (for 127 mononucleotides and mononucleosides).

C1′−C2′−C3′ and O4′−C1′−C2′ angles show any chemically dependent differences.

The valence angles are more dependent on conformational state than on sugar type. The angles in ribose sugars that show conformationally dependent differences include C3′−C4′−O4′, O4′−C1′−C2′, C1′−C2′−O2′, C3′−C2′−O2′, C2′−C3′−O3′, C4′−C3′−O3′, C5′−C4′−C3′, C5′−C4′−O4′, C2′−C1′−N1/N9, and C1′−N1−C2. In deoxyribose sugars, the following angles depend on whether the conformation is C2′- or C3′-*endo*: C2′−C3′−C4′, C3′−C4′−O4′, O4′−C1′−C2′, C2′−C3′−O3′, C4′−C3′−O3′, and C5′−C4′−C3′ (Table 4 (bottom)). These results confirm the periodic sinusoidal dependence of the values of the C3′−C4′−O4′, O4′−C1′−C2′, C4′−O4′−C1′, and C1′−C2′−C3′ endocyclic sugar valence angles with *P* predicted on the basis of a smaller set of molecular structures.[12] The data also confirm the variation of the internal bond angles reported previously[20] as a function of both *P* and the amplitude ν_{max}.

The angles generally agree with those reported by Arnott and Hukins.[11] The present survey, however, finds new conformationally dependent differences in valence angles C5′−C4′−C3′, C5′−C4′−O4′, and C2′−C1′−N1/N9 not evident in the more limited earlier sample. The largest conformationally dependent differences in exocyclic bond angles found previously at the C2′ and C3′ atoms still persist in the present data.

Valence Geometry of the Phosphodiester Linkage. Bond Lengths. The distribution histograms of bond lengths in the phosphodiester linkage are shown in Figure 4, and the statistics of these bond lengths are detailed in Table 5. The P−O5′ bond is shorter than P−O3′. The values for all organic molecules[16] are equivalent to the value found for the P−O3′ bond, and the values found for non-nucleotide phosphodiester containing compounds[14] are close to the value for the P−O5′ bond. Further analysis shows that the O5′−C5′ bond length depends on whether the oxygen is linked to phosphorus or hydrogen.[7] The mean value of O5′−C5′ is 1.422 Å for the terminal HO−C5′ bonds observed in mononucleosides versus 1.440 Å when attached to the phosphate group in dinucleoside phosphates. This latter value is more relevant to nucleic acids and in agreement

Table 5. Bond Lengths and Angles in the Phosphodiester Linkage in Dinucleoside Monophosphates and Trinucleoside Diphosphates[a]

bond	$\bar{x}$	$\bar{x}_A$	$\bar{x}_K$	σ,N	σ_A,N	σ_K,N
P−O1P/O2P[b]	1.485	1.483	1.486	0.017, 30	0.008, 16	0.010, 6
P−O3′	1.607	1.608	1.588	0.012, 13	0.013, 16	0.009, 6
P−O5′	1.593	1.608	1.588	0.010, 15	0.013, 16	0.009, 6
(P)O5′−C5	1.440	1.426	1.442	0.016, 14	0.019, 236	0.012, 6
(P)O3′−C3′	1.433	na	1.442	0.019, 13	na	0.012, 6

angle	$\bar{x}$	$\bar{x}_K$	σ,N	σ_K,N
O1P−P−O2P	119.6	118.9	1.5, 15	0.9, 3
O5′−P−O1P/O2P$_{large}$[c]	110.7	113.4	1.2, 16	1.4, 6
O5′−P−O1P/O2P$_{small}$[d]	105.7	105.5	0.9, 16	2.2, 6
O3′−P−O5′	104.0	105.4	1.9, 13	0.7, 3
P−O5′−C5′	120.9	120.1	1.6, 15	1.2, 6
C3′−O3′−P	119.7	120.8	1.2, 13	2.3, 8
O3′−P−O1P/O2P$_{large}$[c]	110.5	113.4	1.1, 13	1.4, 6
O3′−P−O1P/O2P$_{small}$[d]	105.2	105.5	2.2, 13	2.2, 6
(P)O5′−C5′−C4′	109.4	na	0.8, 14	na
(P)O3′−C3′−C4′	109.3	na	1.5, 13	na

[a] $\bar{x}$, mean value (Å); $\bar{x}_A$, mean value (Å) given by Allen *et al.*;[16] $\bar{x}_K$, mean value (Å) given by Kabelac *et al.*;[14] σ, esd; σ_A, esd of Allen *et al.* parameter; σ_K, esd of Kabelac *et al.* parameter; N, sample size; $\bar{x}$, mean value (deg); $\bar{x}_K$, mean value (deg) given by Kabelac et al.[14] [b] Combined value of P−O1P and P−O2P. [c] Geometries for the subset with large Ox−P−O1P/O2P angles, where x = 3′ or 5′ (see Figure 6). [d] Geometries for the subset with small Ox−P−O1P/O2P angles, where x = 3′ or 5′ (see Figure 6).

with a survey of the valence geometry of all oligonucleotides.[23] The mean value of the O3′−C3′ bond length does not appear to depend on whether the oxygen is bound to phosphorus or hydrogen but does depend on the sugar puckering as shown in Table 3.

Valence Angles. The distributions of the phosphate bond angles are shown in the histograms of Figure 6; other statistics are in Table 5 (bottom). The distribution of the O−P−OP angles linking the main chain oxygen atoms (O) and the side group oxygen atoms (OP) is clearly bimodal as evident from the two very different values for this angle in Table 5 (bottom). The observed bimodality also exists in the histograms where the angles O−P−O1P and O−P−O2P have been separated according to their stereochemistry as defined by the standard IUBMB nomenclature.[24] Thus, the differences in the angles are not due to a configurational effect. The dependence of this angle on either charge or conformation needs to be investigated further.

Significantly different mean values are observed for the O5′−C5′−C4′ angle in different chemical environments. The angle decreases from 111.3° for (H)O5′−C5′−C4′ in mononucleosides to 109.4° for (P)O5′−C5′−C4′ in dinucleoside monophosphates. In contrast, the C4′−C3′−O3′ angle depends only on sugar conformation and not on its oxygen links.

Conformational Analysis of the Sugar−Phosphate Backbone. The observed torsion angles in the survey are summarized in Tables 6 and 7 and Figures 8 and 9. One goal of this analysis was to determine target values for the various torsion angles that could be used in crystallographic refinement. Thus, it was necessary to identify clusters of angles as well as the mean values associated with different conformational ranges.

Ring Torsions. The endocyclic torsion angles $\nu_0-\nu_4$ define the pseudorotation phase angle P (Figure 2). The scattergrams of these torsion angles versus P (Figure 9) confirm the expected sinusoidal variation[5] and the clear preference of the sugar ring for the C2′-*endo* and C3′-*endo* states. The size of the sample presented in this study is large enough so that the data points fit the predicted functions remarkably well. The mean amplitude deduced from the sinusoidal variation of the $\nu_0-\nu_4$ torsion angles versus pseudorotation phase angle P, depicted in Figure 9, is 38.2°. This value is slightly greater than the mean values of ν_{max} (35.2° for deoxyribose and 37.10° for ribose) determined for individual structures calculated using the formula shown in Figure 2.

Scatter charts of the exocyclic sugar torsion angles—C5′−C4′−C3′−C2′, C5′−C4′−C3′−O3′, O4′−C4′−C3′−O3′, C4′−O4′−C1′−N1/N9, and O3′−C3′−C2′−O2′—versus P (Figure 9) also demonstrate a dependence on sugar conformation. Sinusoidal trends not predicted by theory are recognizable for the first four angles. Although the amplitudes of the functions show a broader range, 25°−42°, than those for the five endocyclic ring torsion angles, the average value of 36.5° is still comparable to the calculated values of ν_{max} for all structures.

Statistical tests were performed to see if there are significant conformational differences between deoxyribose and ribose sugars within the C2′-*endo* and C3′-*endo* groups (Table 6). The torsion angles ν_1, ν_2, C5′−C4′−C3′−O3′ (δ), and O4′−C4′−C3′−O3′ are significantly different in C2′-*endo* ribose and deoxyribose sugars and the ν_3, ν_4, C5′−C4′−C3′−C2′, and C4′−O4′−C1′−N1/N9 torsion angles in C3′-*endo* rings.

Glycosyl Torsions. The glycosyl torsion angle χ linking the sugar and base groups, O4′−C1′−N1−C2 for pyrimidines and O4′−C1′−N9−C4 for purines, is bimodal. The range between 170° and 280° is designated as *anti*, and the range between 0° and 100° is designated as *syn*.[25] The scatter chart of χ versus P (Figure 9) shows three clusters of states which reflect the interdependence of two bimodally distributed parameters: *anti* and *syn* base orientations and C2′-*endo* and C3′-*endo* sugar puckers. The C3′-*endo* puckering mode is coupled with *anti* base orientation while the C2′-*endo* sugars adopt both *anti* and *syn* base orientations. There are only two structures with the C3′-*endo/syn* combination (Figure 9), which is known to be sterically hindered.[26] The C2′-*endo/syn* group contains mainly purine nucleosides (20 out of 23). Purines and pyrimidines are equally distributed in the C2′-*endo/anti* and C3′-*endo/anti* groups. These results confirm earlier studies.[5,27]

Backbone Torsions. The values for the backbone torsion angles in this sample are given in Table 6 and their distributions in Figure 8. The rotation about the exocyclic C4′−C5′ bond, designated by the torsion angle γ, describes the position of the 5′-oxygen relative to the sugar. All three classical staggered conformations— +*sc*, −*sc*, and *ap*—are observed in the structures included in this study (Figures 8 and 9). The +*sc*, or +*gauche* conformer shows the highest frequency consistent with its observed preference in solution studies. The mean values of γ reported in Table 7 are based on the following angular clustering: +*sc* (+*gauche*), 30° ≤ γ ≤ 80°; *ap* (*trans*), 160° ≤ γ ≤ 190°; −*sc* (−*gauche*), 280° ≤ γ ≤ 320°.

The sample size for determining the torsion angles at the phosphodiester linkage is small. Nevertheless, the distributions are reasonably clear. The histogram of the α (O3′−P−O5′−C5′) phosphodiester torsion angle is bimodal with conformers in both the +*sc* and −*sc* regions (Figure 8). The ζ distribution of C3′−O3′−P−O5′ angles is more diffuse with a small population in the −*sc* range, another in the +*sc* region, and two contributors to the *ap* region state. The α values are in the

(23) Schneider, B.; Neidle, S.; Berman, H. B. Manuscript in preparation.
(24) Liebecq, C. *Compendium of Biochemical Nomenclature and Related Documents,* 2nd ed.; Portland Press: London and Chapel Hill, 1992.
(25) Saenger, W. *Principles of Nucleic Acid Structure*; Springer-Verlag: New York, Berlin, Heidelberg, Tokyo, 1983.
(26) Olson, W. K. *Biopolymers* **1973**, *12*, 1787−1814.
(27) Haschemeyer, A. E. V.; Rich, A. *J. Mol. Biol.* **1967**, *27*, 369−384.

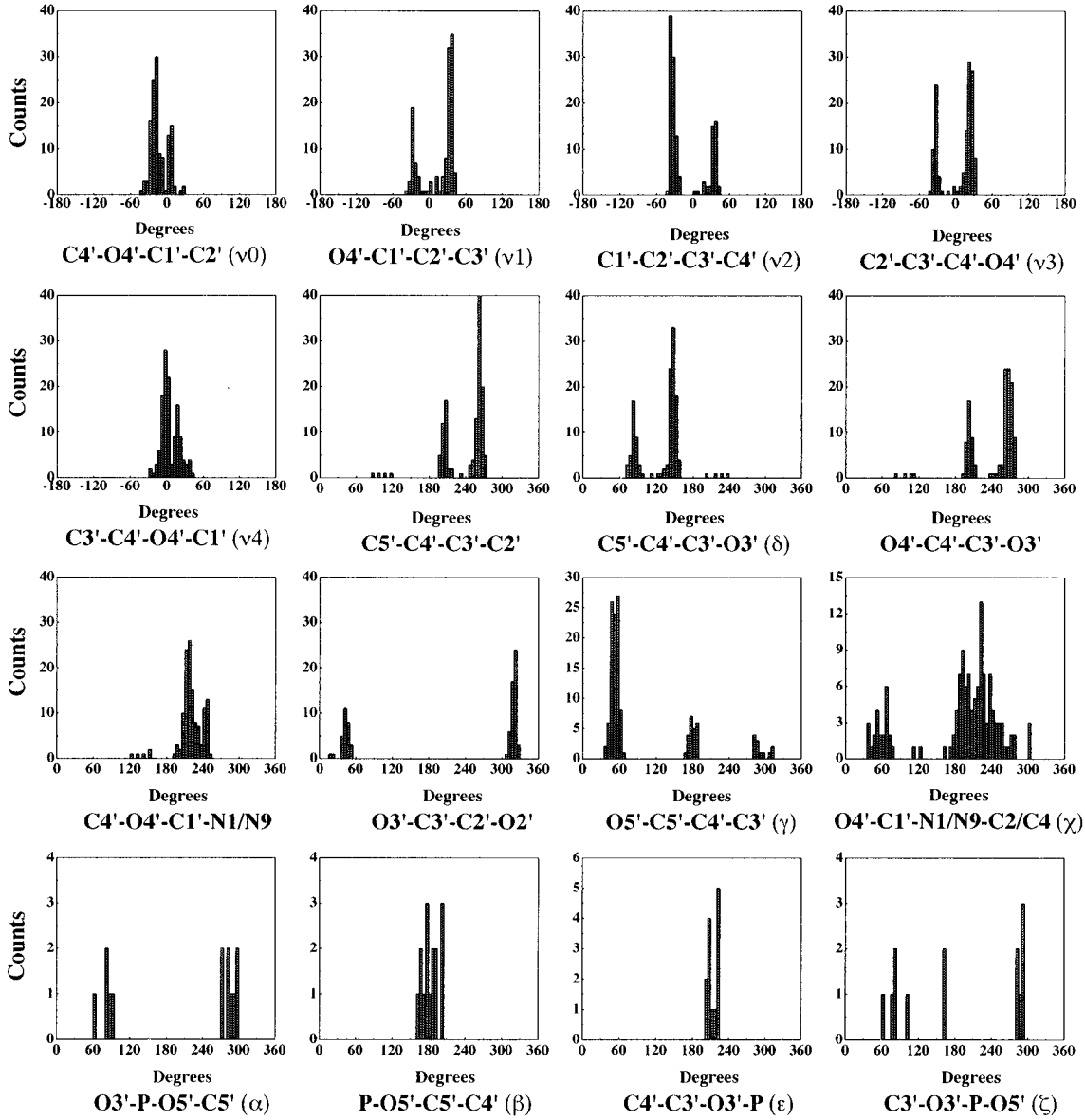

Figure 8. Histograms, in 5° intervals, of torsion angles in the sugar ring and in the phosphodiester linkage. The distributions of torsion angles in the sugar ring are based on 127 mononucleotide and mononucleoside structures. The torsions involving phosphorus are based on 10 di- and trinucleotides.

energetically most favored regions as originally proposed by Newton[28] while the *ap* population of ζ is close to the calculated position of the saddle point. The torsion angle β shows a broad distribution centered at the *ap* position corresponding to the main population of torsion angles in nucleic acid structures. In mononucleotides, the mean value is 20° lower than in dinucleoside phosphates. The ϵ distribution of C4′−C3′−O3′−P falls in a narrow range centered around 220°, similar to what is observed in many right-handed DNA structures. The state near 270° reported in Z-DNA oligonucleotide structures[23] is not represented in this limited high-resolution sample.

Discussion

The preceding analysis contains the best estimates of sugar−phosphate geometry in well-determined crystal structures of low molecular weight nucleic acid analogs. The accumulated data allow for the construction of updated dictionaries that can be used for crystallographic refinement and molecular modeling studies.

Because the sample of mononucleosides and mononucleotides is three times larger than in previous studies, it has been possible to distinguish differences in ribose and deoxyribose sugars separated according to conformational types.

This analysis has revealed other results that were also previously undetectable:

(1) The lengths of all endocyclic bonds and the C3′−O3′ exocyclic bond are different for ribose and deoxyribose structures. The presence or absence of the O2′ hydroxyl atom also changes numerous nearby and distant bond angles, including C1′−C2′−C3′, C2′−C3′−C4′, C5′−C4′−C3′, C2′−C1′−N1/N9, and O4′−C1′−N1/N9.

(2) The mean puckering amplitude ν_{max} of deoxyribose sugars differs from that of ribose rings.

(3) The predicted dependencies of the C3′−O3′ and the C2′−O2′ bond lengths on sugar conformation have been observed as well as a new conformational dependence for C3′−C4′. The previously expected conformational dependencies of the endocyclic sugar valence angles are now revealed. Newly

(28) Newton, M. D. *J. Am. Chem. Soc.* **1973**, *95*, 256−258.

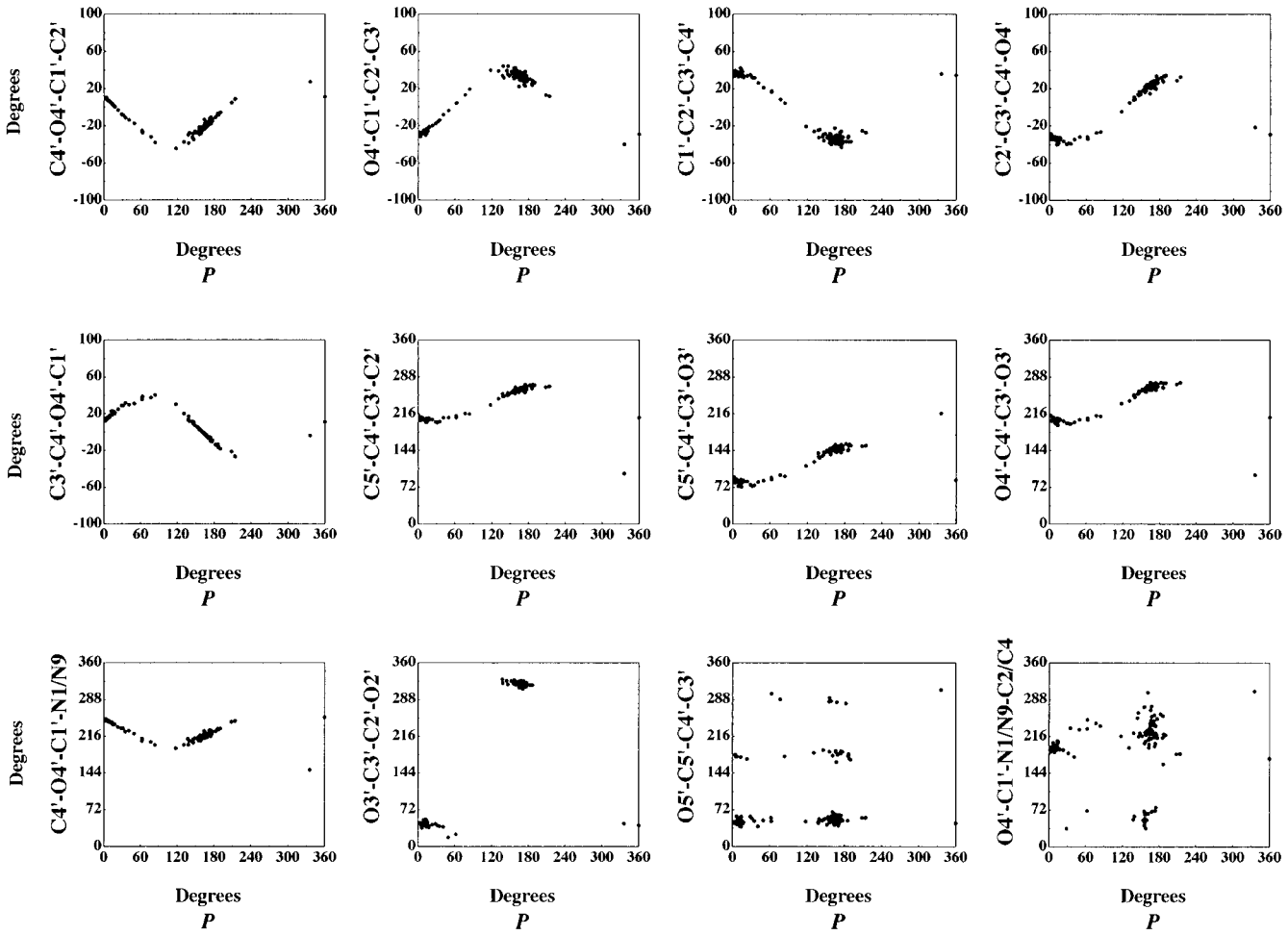

Figure 9. Scattergrams of sugar torsion angles, in degrees, versus pseudorotation phase angle *P*, in degrees (for 127 mononucleotides and mononucleosides).

Table 6. Comparisons of Torsion Angles in Furanose Rings[a]

	C2′-*endo*					C3′-*endo*				
torsion angle	$\bar{x}_R$	$\bar{x}_D$	$P_{t\,C2'}$	σ_R, N	σ_D, N	$\bar{x}_R$	$\bar{x}_D$	$P_{t\,C3'}$	σ_R, N	σ_D, N
C4′−O4′−C1′−C2′ (ν_0)	339.2	340.7	0.297	5.2, 49	6.3, 27[b]	2.8	6.6	0.060	6.1, 24	3.1, 5
O4′−C1′−C2′−C3′ (ν_1)	35.2	32.8	0.029	3.4, 49	4.9, 27	335.4	333.3	0.142	4.9, 24	2.1, 5
C1′−C2′−C3′−C4′ (ν_2)	324.6	326.9	0.006	2.8, 49	3.6, 27	35.9	35.6	0.717	2.8, 24	1.3, 5
C2′−C3′−C4′−O4′ (ν_3)	24.2	22.6	0.141	4.4, 49	4.5, 27	324.7	327.7	0.035	3.1, 24	2.3, 5
C3′−C4′−O4′−C1′ (ν_4)	357.7	357.7	1.000	5.7, 49	6.1, 27	20.5	16.4	0.045	5.1, 24	3.2, 5
C5′−C4′−C3′−C2′	263.4	262.0	0.160	4.1, 49	4.1, 27	204.0	207.0	0.029	3.1, 24	2.2, 5
C5′−C4′−C3′−O3′ (δ)	147.3	145.2	0.048	4.9, 49	4.0, 27	81.0	84.8	0.140	4.4, 24	4.5, 5
O4′−C4′−C3′−O3′	268.1	265.8	0.044	5.3, 49	4.3, 27	201.8	205.4	0.170	4.2, 24	4.8, 5
C4′−O4′−C1′−N1/N9	216.6	217.7	0.470	5.5, 49	6.7, 27	241.4	245.6	0.024	6.5, 24	2.5, 5
O3′−C3′−C2′−O2′	319.7	na	na	4.2, 49	na	44.3	na	na	4.5, 24	na
	$\bar{x}_{C2'}$			$\sigma_{C2'}$, N		$\bar{x}_{C3'}$			$\sigma_{C3'}$, N	
O4′−C1′−N1−C2[c] (χ) (*anti*)	229.8			18.4, 38		195.7			6.6, 16	
O4′−C1′−N1−C2[c] (χ) (*syn*)	63.4			10.2, 2		na			na	
O4′−C1′−N9−C4[d] (χ) (*anti*)	237.0			24.3, 18		193.3			14.0, 12	
O4′−C1′−N9−C4[d] (χ) (*syn*)	58.6			12.0, 15		35.6			0.0, 2	
	$\bar{x}$			σ, N						
O5′−C5′−C4′−C3′ (γ) (−*sc*)	292.9			12.3, 12						
O5′−C5′−C4′−C3′ (γ) (*ap*)	179.4			6.4, 22						
O5′−C5′−C4′−C3′ (γ) (+*sc*)	52.5			5.7, 93						

[a] $\bar{x}_R$, mean value (deg) of ribose torsion angle; σ_R, esd of ribose torsion angle; $\bar{x}_D$, mean value (deg) of deoxyribose torsion angle; σ_D, esd of deoxyribose torsion angle; $\bar{x}_{C2'}$, mean value (deg) of torsion angle χ for C2′-*endo* conformers; $\sigma_{C2'}$, esd of torsion angle χ for C2′-*endo* conformers; $\bar{x}_{C3'}$, mean value (deg) of torsion angle χ for C3′-*endo* conformers; $\sigma_{C3'}$, esd of torsion angle χ for C3′-*endo* conformers; $\bar{x}$ mean value (deg) of torsion angle γ; σ − esd of torsion angle γ; $P_{t\,C2'}$, significance of *t* test for comparison of C2′-*endo* sugars; $P_{t\,C3'}$, significance levels of *t* test for comparison of C3′-*endo* sugars; *N*, sample size. [b] Structures doxadm and jubvil were omitted from the final analysis due to strong deviations. [c] Pyrimidine. [d] Purine.

detected differences are found for several exocyclic angles including C1′−C2′−O2′, C5′−C4′−C3′, C5′−C4′−O4′, and C2′−C1′−N1/N9 in ribose sugars and C5′−C4′−C3′ in deoxyribose sugars.

Table 7. Torsion Angles in the Phosphodiester Linkage in Dinucleoside Monophosphates and Trinucleoside Diphosphates[a]

torsion angle	$\bar{x}$	σ	N
O3′−P−O5′−C5′ (α) (−*sc*)	285.3	9.8	5
O3′−P−O5′−C5′ (α) (+*sc*)	81.0	12.1	8
P−O5′−C5′−C4′ (*β*)	183.5	13.0	15
P−O5′−C5′−C4′ [b] (*β*)	163.8	23.0	24
C4′−C3′−O3′−P (*ϵ*)	214.0	8.6	13
C3′−O3′−P−O5′ (*ζ*) (−*sc*)	289.2	4.8	6
C3′−O3′−P−O5′ (*ζ*) (*ap*)	163.1	0.6	2
C3′−O3′−P−O5′ (*ζ*) (+*sc*)	80.7	14.3	5

[a] $\bar{x}$, mean value (deg) of torsion angle; σ, esd of torsion angle; N, sample size. [b] Parameters found for mononucleotides.

(4) The mean O5′−C5′−C4′ bond angle depends on its chemical environment (i.e., whether the O5′ atom is linked to a phosphorus or a hydrogen). No such difference is found for the O3′−C3′−C4′ angle.

(5) The predicted sinusoidal relationships between the endocyclic sugar torsion angles and the pseudorotation parameter P are now clearly demonstrated.

We feel confident that the results for the sugar rings are statistically meaningful and that the values that are observed for the valence angles and distances and for the conformational states will give useful parameters for crystallographic refinement and molecular modeling. Because of the much smaller sample size, the values for the phosphodiester linkage are not as well determined. This highlights the need for very high resolution crystal structure analyses of oligonucleotides to provide standards for lower resolution studies.

Acknowledgment. This work was supported by a grant from the NSF (BIR 9305135) for the Nucleic Acid Database Project. We thank Christine Zardecki for her help in preparing this paper.

JA9528846